Removal of methylene blue from aqueous solution using Mg-Fe, Zn-Fe, Mn-Fe layered double hydroxide

Zhongliang Shi, Yanmei Wang, Shuyu Sun, Cheng Zhang and Haibo Wang

ABSTRACT

Layered double hydroxides (LDH) with highly flexible and adjustable chemical composition and physical properties have attracted tremendous attention in recent years. A series of LDH with different M (Mg, Zn, Mn)-Fe molar ratios were synthesized by the double titration co-precipitation method. The effect of the factors, including M (Mg, Zn, Mn) : Fe molar ratio, pH, and M-Fe LDH dosage, on the ability of the prepared M-Fe LDH to remove cationic methylene blue (MB) dye from aqueous solution were investigated. Results indicated that the removal efficiency of MB (10 mg/L) was the best at the M (Mg, Zn, Mn): Fe molar ratio of 3:1 by using 2.0 g/L of M-Fe LDH at pH 6.0 under 298.15 K. Mg-Fe LDH had the highest removal performance (71.94 mg/g at 298.15 K) for MB compared to those of the Zn-Fe and Mn-Fe LDH. Zn-Fe LDH with the smallest activation energy resulted in the fastest adsorption rate of MB. The pseudo-second-order model and Langmuir adsorption isotherm were also successfully applied to fit the theory of M-Fe LDH for removal of MB.

Key words | methylene blue, Mg-Fe LDH, Mn-Fe LDH, Zn-Fe LDH

Zhongliang Shi
Yanmei Wang
Shuyu Sun
Cheng Zhang
Haibo Wang (corresponding author)
Liaoning Engineering Research Center for Treatment and Recycling of Industrially Discharged Heavy Metals,
Shenyang University of Chemical Technology,
Shenyang 110142,
China
E-mail: *wanghaibo@syuct.edu.cn*

Haibo Wang
College of Environmental and Safety Engineering,
Shenyang University of Chemical Technology,
Shenyang 110142,
China

HIGHLIGHTS

- Mg-Fe, Zn-Fe, Mn-Fe layered double hydroxide were successfully prepared by double titration co-precipitation method.
- The maximum adsorption capacity of Mg-Fe LDH was 71.94 mg/g at 298.15 K.
- The pseudo-second-order model fit the theory of M-Fe LDH for removal of MB.
- The Langmuir adsorption isotherm was also successfully applied.
- Zn-Fe LDH, with the smallest activation energy, resulted in the fastest adsorption rate of MB.

INTRODUCTION

With rapid economic development, the water environment is facing a more and more serious situation, the water pollution problems have become one of the most difficult environmental problems (Yang *et al.* 2019). One of the important reasons for water pollution is the discharge of dyeing wastewater, which will pollute groundwater sources, and thus cause serious harm to human health (Pan *et al.* 2019; Liang *et al.* 2020). Dyes in wastewater are normally the result of inefficient dyeing processes, which cause as much as 10–15% unused dyestuff entering the watercourse directly (Selvam *et al.* 2003). Dye effluent normally contains about 10–50 mg/L (Zollinger 1989; Lazaridis *et al.* 2003), and thus may be perceived as being contaminated and unacceptable. Methylene blue (MB) is a representative phenothiazine type cationic dye, which is usually used in the dyeing industry (Li *et al.* 2018). MB is toxic to humans and animals, especially aquatic organisms (Thi *et al.* 2020), and needs to be effectively removed from dyeing wastewater. This poses a challenge to remove MB methods from dyehouse effluent.

Several methods have been employed to deal with dyeing wastewater, such as coagulation (Khorram & Fallah 2018), chemical precipitation (Hua *et al.* 2014), ozonation (Hu *et al.* 2016), membrane filtration (Rashidi *et al.* 2014)

doi: 10.2166/wst.2020.313

and reverse osmosis (Lee *et al.* 2020). Besides, the adsorption technique is regarded as the most effective technique for MB removal from dyeing wastewater as a result of its simplicity in design, relatively low cost and high efficiency (Altintig *et al.* 2017; Islam *et al.* 2017). The use of the synthetic anionic clays such as hydrotalcite (HT) or hydrotalcite-like compounds (HTlc) or layered double hydroxide (LDH) for adsorptive removal of dyes present in aqueous effluents has attracted great attention recently (Zhou *et al.* 2011; Lan *et al.* 2014; Chowdhury & Bhattacharyya 2015). In recent years, there have been significant amounts of work on the application of LDH to remove MB (Chuang *et al.* 2008; Wang *et al.* 2013; Kalalie *et al.* 2016). For example, Zhao *et al.* (2017) have reported Mg-Al-LDH, which was synthesized by using a hydrothermal method and acted as a sorbent for the removal of MB from aqueous solution; the adsorption capacity of Mg-Al-LDH at 298.15 K could reach up to about 20 mg/g. Bi & his co-workers (2011) developed heteropoly blue-intercalated layered double hydroxide (HB-LDH) by the ion-exchange method as an adsorbent for removal of MB and the maximum adsorption capacity of MB was 30.87 mg/g. Xia *et al.* (2014) observed the removal efficiency for MB by three Ti-based layered double hydroxides under visible light, which followed the order: CeO_2/Zn-Ti LDHs > Zn/Al-Ti/SB LDHs > Zn/Ti LDHs. In this study, the M-Fe LDH was selected as the material of adsorbent to remove MB. This reason was that M-Fe LDH had layered structure, a large specific surface area, strong ion exchange performance and low cost.

In this paper, the double titration co-precipitation method was used to synthesize the Mg-Fe LDH, Zn-Fe LDH, and Mn-Fe LDH, that method provided better crystallinity and better control of the particle size (Yu *et al.* 2015; Bukhtiyarova 2019). The microscopic morphological characteristics and structural information of M(Mg, Zn, Mn)-Fe LDH were investigated by using the BET method, FT-IR, SEM, and XRD technology. Effect of M (Mg, Zn, Mn) : Fe molar ratio, pH, and M-Fe LDH dosage on the removal of MB were studied. Moreover, adsorption kinetics, adsorption thermodynamics, and adsorption isotherms were also conducted to fit the theory of M-Fe LDH for removal of MB.

EXPERIMENTAL

All the chemicals used in the study are of analytical grade. All the solutions in the study were prepared using de-ionized water.

The preparation of the adsorbents was carried out by the method of co-precipitation. The 0.675 mol of NaOH and 0.225 mol of Na_2CO_3 were dissolved in 250 mL of de-ionized water to make a base solution. Then 0.045 mol of $MgCl_2$ ($ZnCl_2$ or $MnCl_2$) and 0.015 mol of $FeCl_3{\cdot}4H_2O$ are added into 100 mL of de-ionized water to make the metal salt solution. The base solution and metal salt solution were added dropwise to 10 mL of de-ionized water, and the pH of this process maintained at 8–10. The filtrate was filtered and washed with excess water, then dried at 353.15 K for 24 h. This sample was denoted as Zn-Fe LDH, and Mg-Fe LDH or Mn-Fe LDH.

In order to investigate the effect of M (Mg, Zn, Mn) : Fe molar ratio on the removal of MB, a series of parallel experiments were carried out at different M (Mg, Zn, Mn) : Fe molar ratios (1:1, 2:1, 3:1, 4:1, and 5:1) for the removal of 10 mg/L MB (25 mL) at 298.15 K for 30 min. To investigate the effect of M-Fe LDH dosage on the removal of MB, a series of parallel experiments was carried out at different M-Fe LDH dosage (0.4, 0.8, 1.2, 1.6, 2.0, 2.4 g/L) for the removed of 10 mg/L MB (25 mL) at 298.15 K for 30 min.

The effect of pH on MB removal was also studied on the 10 mg/L of MB solutions (pH 6.3) at the pH range from 2 to 12 with 2.0 g/L g of adsorbent at 298.15 K for 30 min. The pH values were determined by using a pH-meter and adjusted 0.1 mol/L HCl and 0.1 mol/L NaOH solutions.

The adsorption kinetics experiments were carried out by using 2.0 g/L of M-Fe LDH for removal of 10 mg/L MB (25 mL) at 298.15 K for different time (2, 5, 10, 15, 20, 30, 45, 60, 90, 120 min). The adsorption isotherms experiments were executed by using 2.0 g/L of M-Fe LDH for removal of 25 mL of different concentrations of MB (6, 8, 10, 15, 20, 25, 40, 60, 80, 100 mg/L) at 298.15 K, 308.15 K and 318.15 K, respectively. All experiments were done in duplicate and the average value was used in the evaluation. A blank sample containing no dye and another containing dye solution only were run together with every batch of the sample run.

To conduct the adsorption experiments, a certain amount of M-Fe LDH was added to a 25 mL of MB (10 mg/L) solution at a given pH. The mixture was stirred at a given temperature for 30 min. Then the samples were centrifuged at 7,000 r/min for 30 min. The supernatant was sampled and diluted in the linear range. The sample was analyzed by using an ultraviolet and visible spectrophotometer (TU 1810 pc, Beijing Purkinje General Instrument Co.) at 665 nm (λ_{max} of MB) to determine the residual MB concentration. The pH of solution was measured with a pH meter using a combined glass electrode.

The Fourier transform infrared spectroscopy (FT-IR) of the samples were collected on NICOLET 6700 equipment and scanned at 0.05 cm^{-1} resolution between 400 and 4,000 cm^{-1}. The X-ray diffraction (XRD) patterns were obtained on the Bruker AXS D8 Advance with CuKα radiation ($\lambda = 1.5418$ Å). The surface morphology of the adsorbent was observed by used a scanning electron microscope (SEM) on a JSM-6360LV. The Brunauer-Emmett-Teller (BET) surface area, the total pore volume, and pore diameters were analyzed by used a micromeritics SSA-6000 volumetric adsorption analyzer.

The q_e (mg/g) is the adsorption that was calculated using Equation (1):

$$q_e = \frac{(C_0 - C_e)V}{m} \quad (1)$$

where C_0 (mg/L) is the initial concentrations of MB, C_e (mg/L) is the equilibrium concentrations of MB, V (L) is the total volume, and m (g) is the mass of the M-Fe LDH.

RESULTS AND DISCUSSION

Effect of M (Mg, Zn, Mn) : Fe molar ratio on the removal of MB

The effect of M (Mg, Zn, Mn) : Fe molar ratio on the MB removal efficiency at pH 6.3 is shown in Figure 1. The removal efficiency of MB increased with increased M (Mg, Zn, Mn) : Fe molar ratio from 1:1 to 3:1, but decreased with increased M (Mg, Zn, Mn) : Fe molar ratio from 3:1 to 5:1. When the M/Fe molar ratio is less than 3, the adsorption of MB on M-Fe LDH is limited to the surface electrostatic interaction (Chitrakar *et al.* 2011). Chitrakar *et al.* (2008) proposed that stronger interactions between the charged layers exist in LDH with high charge density (2:1). These interactions reduce the ability of the LDH to expand and accommodate large anions in the interlayer region. In the case where the M/Fe molar ratio is 3, the adsorption of MB on M-Fe LDH includes the electrostatic adsorption on the outer layer cation and the exchange adsorption of the elastic interlayer anions. This is related to the fact that M-Fe LDH (M/Al = 3) allows the formation of the best crystalline LDH phase (Goh *et al.* 2008) for uptake of additional guest species within its interlayers, thus resulting in the highest affinity for MB (Li & Duan 2005). M-Fe LDH synthesized at the M/Fe molar ratio rise 4 and 5 may contain certain amounts of amorphous metal hydroxides, which could potentially results in underestimating the sorption capabilities of M-Fe LDH (Wang & Gao 2006). When the M (Mg, Zn, Mn)/Fe molar ratio was 3:1, the removal efficiency of MB was 82% for Mg-Fe LDH, 58% for Zn-Fe LDH, and 70% for Mn-Fe LDH, respectively. Thus, the optimum molar ratio of M/Fe was 3:1 to wipe off MB.

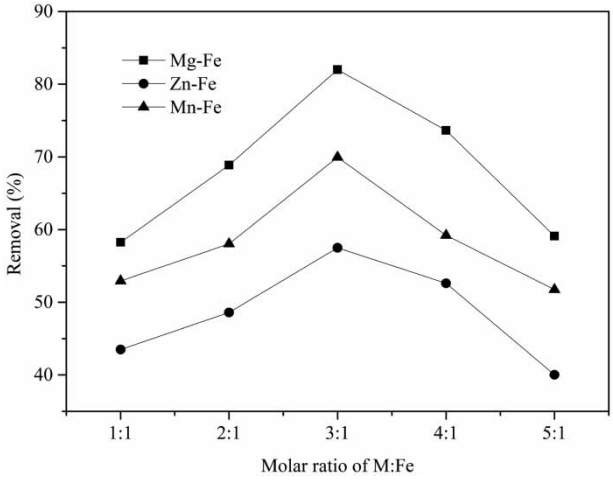

Figure 1 | Effect of M (Mg, Zn, Mn) : Fe molar ratio on the removal of MB.

The microstructure characteristics of the M-Fe LDH at the M (Mg, Zn, Mn)/Fe molar ratio of 3:1 were then evaluated via XRD, SEM, FT-IR, and BET method. Figure 2 shows that the microscopic morphological characteristics of M-Fe LDH adsorbent confirmed by SEM. M-Fe LDH adsorbent was spherical. The particle size of Mg-Fe LDH was bigger than that of Zn-Fe LDH and Mn-Fe LDH. At the same time, the surface of Mg-Fe LDH (Figure 2(a)) was floc distribution and rough, and the pores were staggered, which were favorable for adsorption. However, the surface of Mn-Fe LDH was smooth, which resulted in the smaller specific surface area of the adsorbent. N_2 adsorption-desorption technology was further employed to investigate that the specific surface areas of Mg-Fe LDH, Zn-Fe LDH and Mn-Fe LDH were 104.86, 20.29, 50.49 m^2/g, respectively. N_2 adsorption-desorption results indicated Mg-Fe LDH with the greatest specific surface area. Then SEM results show that the surface of Mg-Fe LDH is flocculent and rough, which can provide a large specific surface area. These results indicate that Mg-Fe LDH will have a greater adsorption capacity for MB.

The FT-IR spectrum and XRD of Mg-Fe LDH, Zn-Fe LDH and Mn-Fe LDH are shown in Figure 3. The results show in the FT-IR spectrum that a broad peak around 3,450 cm^{-1} was associated with stretching vibration of

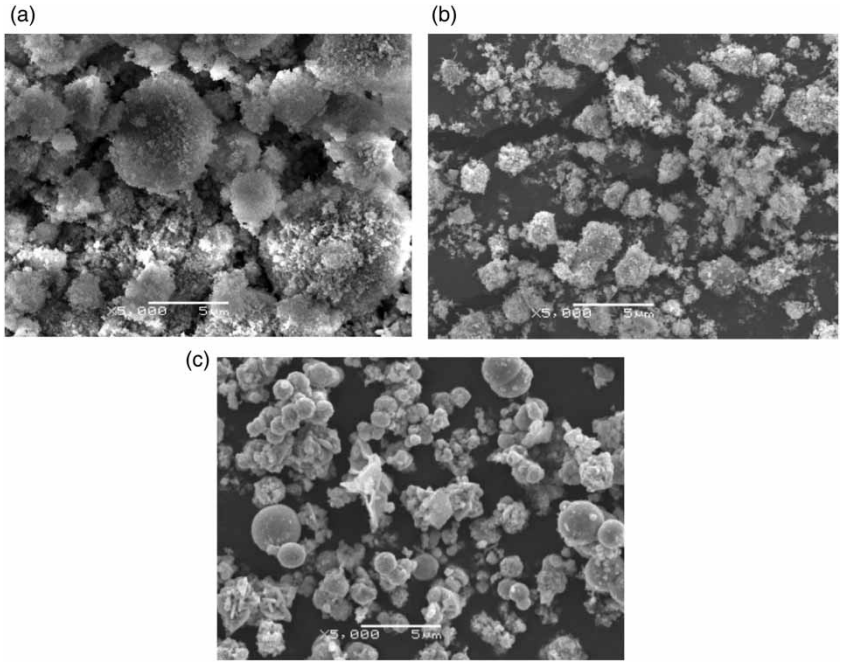

Figure 2 | SEM image of M-Fe LDH adsorbent: (a) Mg-Fe LDH; (b) Zn-Fe LDH; (c) Mn-Fe LDH.

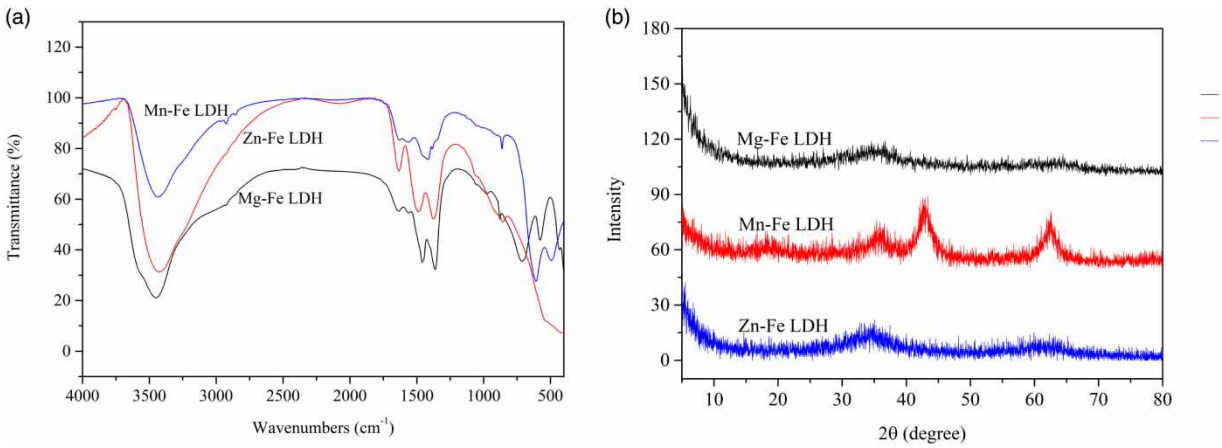

Figure 3 | The FT-IR spectrum (a) and XRD (b) of Mg-Fe LDH, Zn-Fe LDH, and Mn-Fe LDH (the molar ratio of M/Fe = 3:1).

hydrogen-bonded hydroxyl groups from both the hydroxyl group of the layers and interlayer water (Fernandez *et al.* 1998). Sharp peaks around 1,400 cm^{-1} and 1,600 cm^{-1} represented symmetric and asymmetric stretching absorption of the C = O group. Those were typical characteristics for layered double hydroxide materials (Cavani *et al.* 1991). The peaks below 1,000 cm^{-1} correspond to the metal hydrogen bond, and the metal-oxygen stretching mode was represented by peaks between 500 and 800 cm^{-1}. XRD results showed the crystallography and phase information on M-Fe LDH adsorbent. The XRD patterns showed the Mn-Fe LDH was more crystalline than Mg-Fe LDH and Zn-Fe LDH synthesized under the same conditions.

Effect of M-Fe LDH dosage and pH on the removal of MB

Figure 4(a) shows the influence of M-Fe LDH (M:Fe = 3:1) dosage on the removal efficiency of 10 mg/L of MB. These results indicated the removal efficiency of MB increased with an increased M-Fe LDH dosage from 0.4 g/L to 2.0 g/L. The reason is that the number of active sites on the surface of the adsorbent increases as the adsorbent

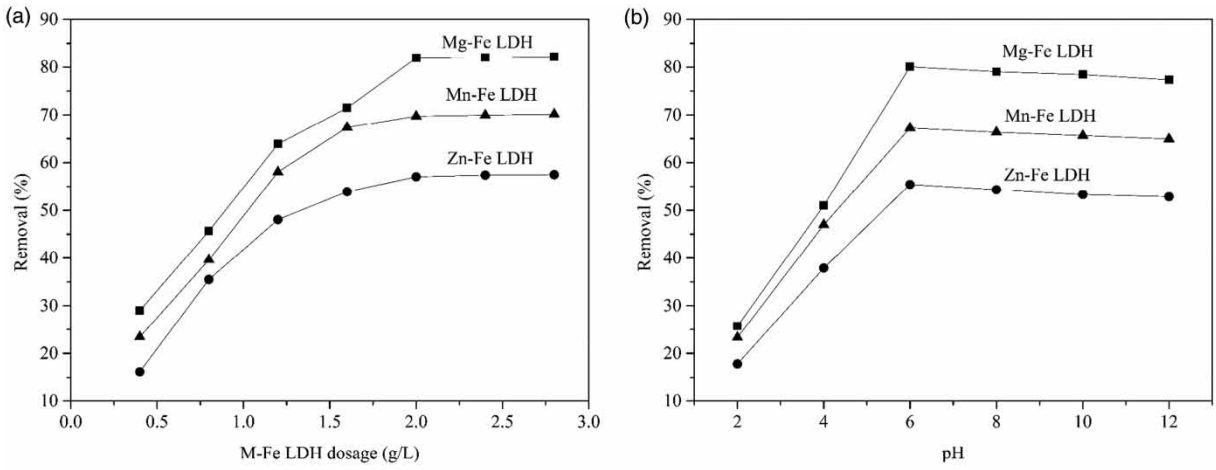

Figure 4 | Effect of M-Fe LDH dosage (a) and pH (b) on the removal of MB.

dosage increases, which causes more MB to be absorbed on the adsorbent, resulting in the removal efficiency increases. However, the removal efficiency of MB at M-Fe LDH dosages between 2.0 g/L and 2.8 g/L maintained the constant of 57% for Zn-Fe LDH, 70% for Mn-Fe LDH, and 81% for Mg-Fe LDH, respectively. At this time, the increasing dosage of absorbents increases the collision rate between particles, and particles aggregate to become the larger particle resulted in decrease of the specific surface area. The change trend between the removal efficiency of MB and the adsorbent dosage is consistent with Abdelkader *et al.*'s research. Abdelkader *et al.* (2011) researched the Orange G amount adsorbed by Mg-Fe LDH increased with increasing adsorbent dose until 1.4 g/L, from this dose the quantities of dye adsorbed on this materials remained unchanged. Hence, the optimum adsorbent dosage of M-Fe LDH on the removal of MB was determined at 2.0 g/L, which were used as the dosage of the following experiments.

The effect of initial pH on the removal efficiency of MB (10 mg/L) was investigated by using 2.0 g/L M-Fe LDH at 298.15 K for 30 min. The results are shown in Figure 4(b) that the maximum efficiency of MB was observed at pH 6.0, which was close to the natural pH of MB solution (6.3). In the solution with lower pH (pH <6.0), H^+ reacted with the metal hydroxyl compound to make the surface positively charged, H^+ and the positively charged MB produced competitive adsorption, so the removal rate was low. OH^- and positively charged MB produce a dark purple precipitate in higher pH (pH > 6.0). Thus, all subsequent experiments on the effect of adsorption variables on MB removal was carried out at pH 6.0.

Adsorption kinetics

The contact time between the pollutant and the adsorbent is an important parameter in adsorption. Figure 5(a) shows the effect of contact time on the adsorption of 10 mg/L MB by using M-Fe LDH adsorbent at 298.15 K. There was the availability of numerous active adsorption sites at the beginning of contact time, which resulted in the adsorption of MB initially increasing rapidly with time. As time progressed, the adsorption of MB reached an equilibrium due to the decreasing number of available active adsorption sites. After the initial adsorption, the rate of MB removal was controlled by the rate of MB transported from the exterior to the interior sites of the adsorbents until all available surface sites were occupied (Kannan & Sundaram 2001; Amin 2008). Mg-Fe LDH showed a much greater adsorption capacity for MB than those of Mn-Fe LDH and Zn-Fe LDH. In this experiment, we use the pseudo-second-order equation (Equation (2)) (Rengaraj *et al.* 2004) to analyze the adsorption kinetics of MB on the M-Fe LDH adsorbent samples. The line plots of t/q_t versus time are shown in Figure 5(b) and the corresponding kinetic parameters are listed in Table 1. The values of R^2 (>0.9999) indicate that MB adsorption is successfully fitted by the pseudo-second-order model.The experimental values of the equilibrium adsorption capacity (q_e^{Exp}) are in close agreement with values of q_e^{Cal} calculated from the pseudo-second-order model. The results of Li *et al.* (2020) and Kumar *et al.* (2010) also indicated the pseudo-second-order kinetic models fitted almost all the process of MB adsorbed onto adsorbents. For the same temperature, the order of reaction

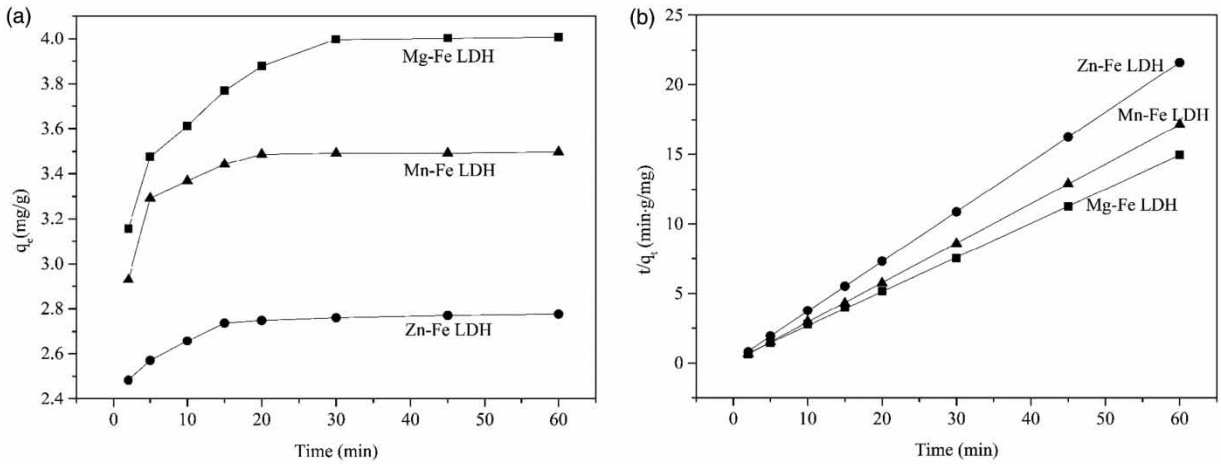

Figure 5 | The effect of contact time on the removal of MB (a); the pseudo-second-order plot for the removal of MB (b).

rate constant is $k_{\text{Mg-Fe}} < k_{\text{Mn-Fe}} < k_{\text{Zn-Fe}}$. It indicates that the adsorption of MB by Zn-Fe LDH is the fastest.

$$\frac{t}{q_t} = \frac{1}{kq_e^2} + \frac{t}{q_e} \tag{2}$$

where k is the adsorption rate constant ($\text{g}\cdot\text{mg}^{-1}\cdot\text{min}^{-1}$), t (min) is time, q_t (mg/g) and q_e (mg/g) are the adsorption capacities at t (min) and at equilibrium.

Adsorption thermodynamics

In order to further study the effect of temperature on the adsorptive capacity of MB onto M-Fe LDH, the adsorption of 10 mg/L MB by using M-Fe LDH adsorbent was carried out at 298.15 K, 308.15 K, and 318.15 K (Figure 6), respectively. The effect of temperature on the pseudo-second-order constants is shown in Figure 6. It is seen from Figure 6 that the pseudo-second-order constant increased with increasing temperature for the same adsorbent. The reason was that the collision probability of the activated sites on the surface of the adsorbent particles increased with increasing temperature resulting in promotion of the adsorption reaction (Salleh *et al.* 2011).

The activation energy (E_a) can be described according to the Arrhenius formula (Equation (3)). The activation energy obtained from the slope of the linear plot of $\ln k$ *vs.* $1/T$ in Figure 7(a). From Table 2, we can see clearly that Zn-Fe LDH with the smallest activation energy results in the adsorption of MB being fastest. The activation entropy and the activation enthalpy of adsorption are calculated using the H. Eyring equation (Futalan *et al.* 2019) shown in Equation (4). ΔS and ΔH are obtained from the intercept and slope of the linear plot of $\ln(k/T)$ *vs.* $1/T$ in Figure 7(b). The negative value of ΔH reflects the exothermic nature of the adsorption process, while the negative value of ΔS reflects reduced randomness in the solid-solution interface during the adsorption process.

$$\ln k = \ln A - \frac{E_a}{RT} \tag{3}$$

$$\ln\frac{k}{T} = -\frac{\Delta H}{R}\times\frac{1}{T} + \ln\frac{k_B}{h} + \frac{\Delta S}{R} \tag{4}$$

Table 1 | The parameters of the pseudo-second-order kinetics model

Adsorbents	Concentration of MB (mg/L)	k	q_e^{Cal} (mg/g)	q_e^{Exp} (mg/g)	R^2	Reference
Mg-Fe LDH	10	0.2648	4.0756	4.0076	0.99992	In this study
Zn-Fe LDH	10	0.9005	2.7949	2.7766	0.99999	In this study
Mn-Fe LDH	10	0.8940	3.5199	3.4978	0.99999	In this study
Graphene aerogel (298 K)	100	0.1033	199.68	200.8 0	0.9999	Li *et al.* (2020)
Cashew nut shell activated carbon (303 K)	100	0.0021	49.485	45.075	0.999	Kumar *et al.* (2010)

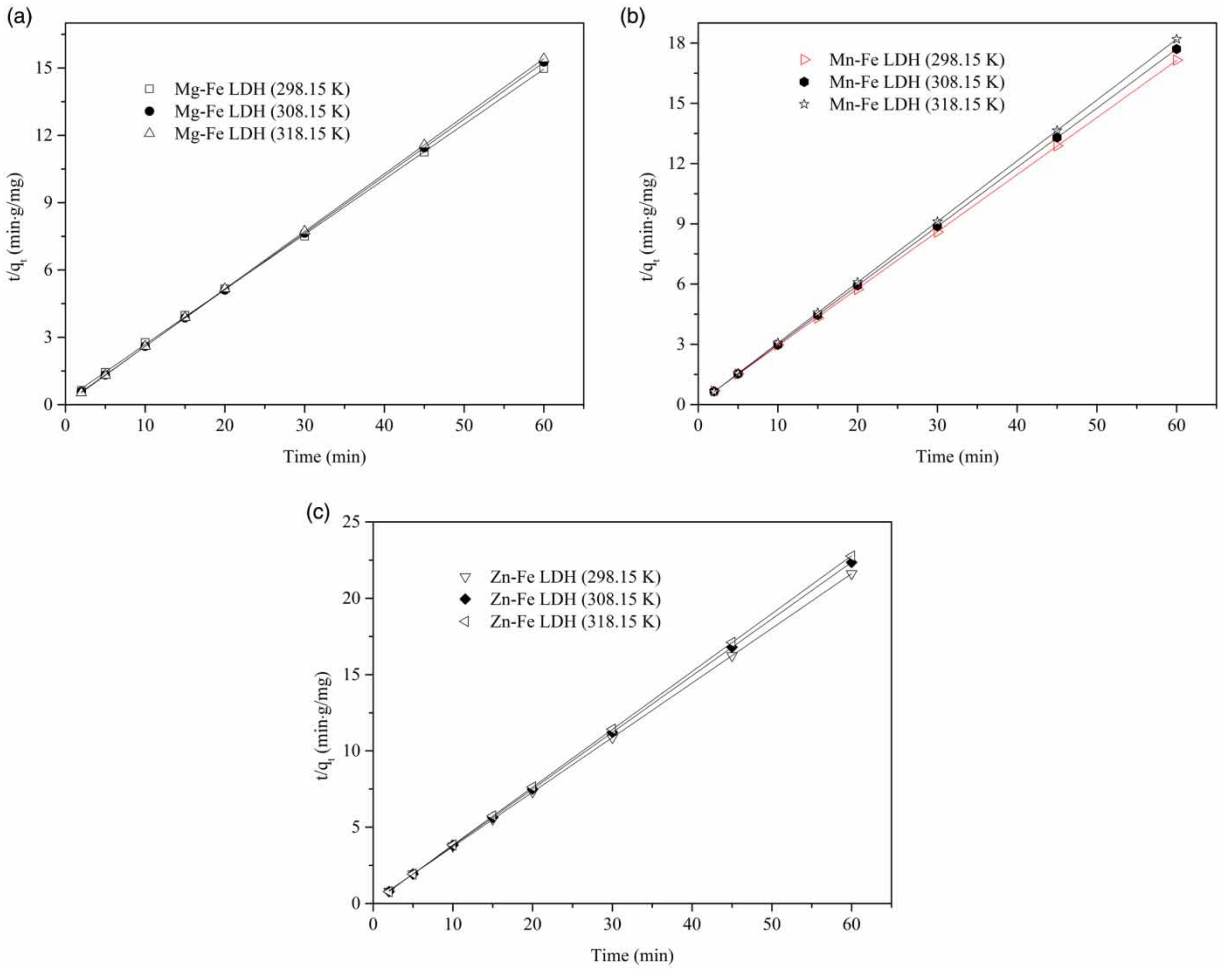

Figure 6 | The effect of temperature on the pseudo-second-order constants.

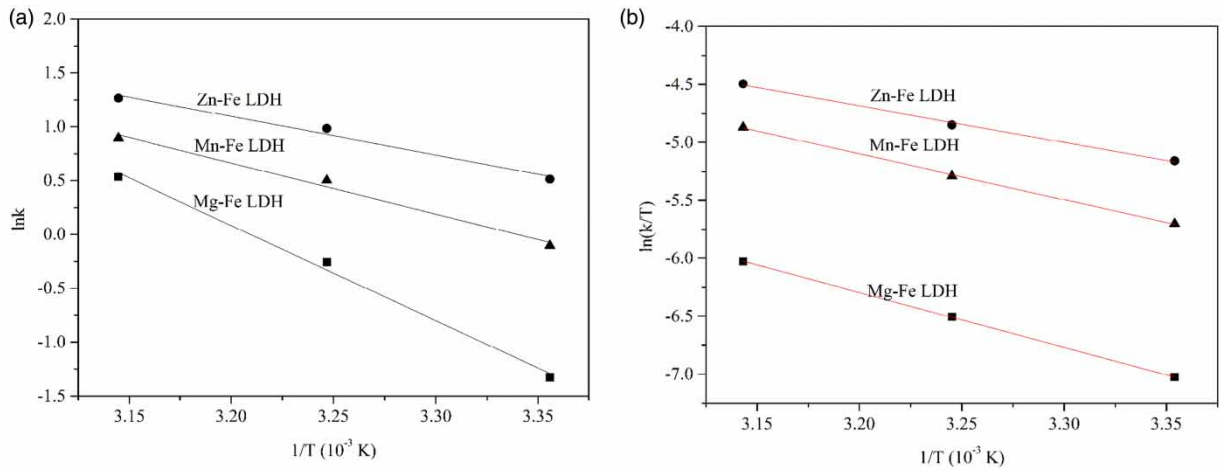

Figure 7 | Relationship between ln*k* (a), ln(*k*/*T*) (b) and 1/*T* for the adsorption of MB by using M-Fe LDH adsorbent.

Table 2 | The activation energy, enthalpy and entropy of M-Fe LDH adsorbent

Sample	Temperature (K)	k	E_a (KJ/mol)	ΔH (KJ/mol)	ΔS (KJ/mol)
Mg-Fe LDH	298.15	0.2648	73.5	− 39.4	− 123.9
	308.15	1.0261			
	318.15	2.5446			
Zn-Fe LDH	298.15	0.8940	29.8	− 26.2	− 152.7
	308.15	1.9802			
	318.15	3.5512			
Mn-Fe LDH	298.15	0.6675	39.5	− 32.9	− 134.7
	308.15	1.6518			
	318.15	2.6465			

where k is the adsorption rate constant (g/(mg/min)), A is the pre-exponential factor, E_a is the activation energy (kJ/mol), R is the molar gas constant (J/(mol·K)), T is the temperature (K); k_B is the Boltzmann constant, h is the Planck constant, ΔS is the activation entropy (kJ/K·mol), ΔH is the activation enthalpy (kJ/mol).

Adsorption isotherms

The purpose of the study is to determine the maximum adsorption capacity of M-Fe LDH adsorbent for MB removal in wastewater. Langmuir and Freundlich adsorption models are usually used to fit the adsorption capacity. Langmuir adsorption isotherm model (Choi 2017) is widely used for the description of the homogeneous adsorption on the surface of the monolayer, Equation (5) is as follows:

$$\frac{C_e}{q_e} = \frac{C_e}{q_m} + \frac{1}{K_L q_m} \tag{5}$$

where q_e is the equilibrium adsorption capacity, q_m is the maximum adsorption capacity, C_e is the concentration of MB after adsorption equilibrium, and K_L is the adsorption constant.

Freundlich isothermal adsorption model (Xie *et al.* 2019) is used to describe the adsorption on heterogeneous surfaces as follows:

$$\lg q_e = \frac{1}{n}\lg C_e + \lg K_F \tag{6}$$

where K_F is Freundlich constant, n is adsorption constant.

Figure 8 shows the adsorption isotherms of M-Fe LDH adsorbent for MB removal at different concentrations and temperatures. It was shown that the adsorption capacity of M-Fe LDH adsorbent for MB decreased with the increase of temperature, which indicated that the reaction was exothermic. The MB equilibrium adsorption increased with an increase in initial MB concentration at the same temperature. Table 3 shows the parameters of the Langmuir

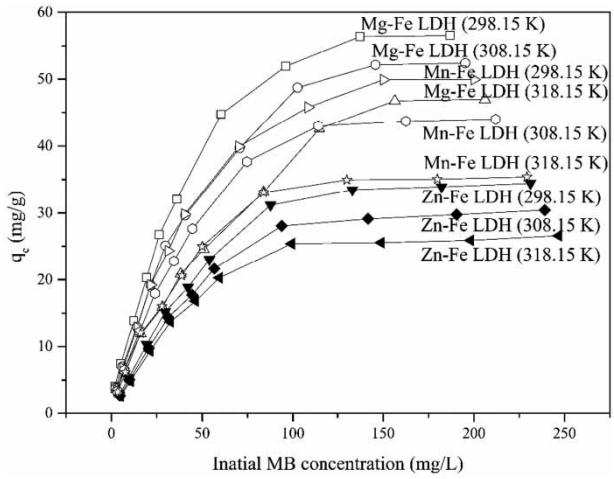

Figure 8 | Adsorption isotherms of M-Fe LDH adsorbent for MB removal at different temperatures.

Table 3 | The parameters of the Langmuir and Freundlich isotherm models

		Langmuir isotherm model			Freundlich isotherm model		
Sample	Temperature (K)	q_m	K_L	R^2	n	K_F	R_2
Mg-Fe LDH	298.15	71.9424	0.02336	0.9944	1.6292	3.0269	0.9858
	308.15	68.4932	0.01965	0.9943	1.5957	2.5067	0.9874
	318.15	64.1026	0.01446	0.9828	1.6067	2.0249	0.9962
Zn-Fe LDH	298.15	45.6221	0.01652	0.9906	1.5291	1.3596	0.9704
	308.15	38.9105	0.01813	0.9925	1.5911	1.3354	0.9661
	318.15	32.8947	0.02079	0.9928	1.6647	1.3363	0.9584
Mn-Fe LDH	298.15	65.7895	0.01903	0.9965	1.5361	2.1577	0.9783
	308.15	56.8182	0.02003	0.9940	1.5748	2.0184	0.9760
	318.15	43.1034	0.02480	0.9953	1.7271	2.0701	0.9697

and Freundlich isotherm model. The correlation coefficient of the Langmuir model was higher than the correlation coefficient of the Freundlich model fitting, which indicated the Langmuir adsorption isotherm equation was more suitable to describe the process of the adsorption on MB by using M-Fe LDH adsorbent. The Langmuir adsorption isotherm model assumes that the adsorbent surface is uniform, the adsorption process is monolayer adsorption. The magnitude of activation energy can indicate whether the adsorption mechanism is physical adsorption (the activation energy of 5–40 kJ·mol^{-1}) or chemical adsorption (the activation energy of 40–800 kJ·mol^{-1}) (Konicki *et al.* 2012). The activation energy value of 73.5 kJ·mol^{-1} indicates that the adsorption of MB onto Mg-Fe LDH is mainly a chemical adsorption process. The value of 29.8 and 39.5 kJ·mol^{-1} for the activation energy indicates that the adsorption of MB onto Zn-Fe LDH and Mn-Fe LDH is mainly a physical adsorption process. The comparison of q_m for MB of Mg-Fe LDH, Zn-Fe LDH, and Mn-Fe LDH adsorbents found that Mg-Fe LDH had a remarkably high adsorption capacity of 71.94 mg/g at 298.15 K.

CONCLUSIONS

In this paper, Mg-Fe, Zn-Fe, and Mn-Fe layered double hydroxide were prepared by double titration co-precipitation method for the removal of MB. The optimal molar ratio of M (Mg, Zn, Mn) : Fe is 3:1 for the removal of MB. The adsorption results exhibited that 2.0 g/L of M-Fe LDH for the removal efficiency of MB (10 mg/L) was best at pH 6.0. The adsorption data of M-Fe LDH samples were well fitted by the Langmuir adsorption isotherm and, moreover, its maximum adsorption capacity of Mg-Fe LDH was 71.94 mg/g at 298.15 K. Besides, the adsorption kinetic study showed that the adsorption of MB onto M-Fe LDH followed the pseudo-second-order kinetic model. Adsorption thermodynamics results showed Zn-Fe LDH, with the smallest activation energy, resulting in its adsorption of MB being the fastest. Then, Mg-Fe LDH could be a cost-effective and promising material for MB removal from the dyeing wastewater.

ACKNOWLEDGEMENTS

This project was supported by the National Key Research and Development Program of China (2017YFD0800301) and the Liaoning Province Natural Science Foundation of China (2020-MS-232).

DATA AVAILABILITY STATEMENT

All relevant data are included in the paper or its Supplementary Information.

REFERENCES

Abdelkader, N. B., Bentouami, A., Derriche, Z., Bettahar, N. & Ménorval, L. C. 2011 Synthesis and characterization of Mg-Fe layer double hydroxides and its application on adsorption of Orange G from aqueous solution. *Chemical Engineering Journal* **169** (1–3), 231–238.

Altintig, E., Altundag, H., Tuzen, M. & Sarı, A. 2017 Effective removal of methylene blue from aqueous solutions using magnetic loaded activated carbon as novel adsorbent. *Chemical Engineering Research and Design* **122**, 151–163.

Amin, N. K. 2008 Removal of reactive dye from aqueous solutions by adsorption onto activated carbons prepared from sugarcane bagasse pith. *Desalination* **223** (1–3), 152–161.

Bi, B., Xu, L., Xu, B. & Liu, X. 2011 Heteropoly blue-intercalated layered double hydroxides for cationic dye removal from aqueous media. *Applied Clay Science* **54** (3–4), 242–247.

Bukhtiyarova, M. V. 2019 A review on effect of synthesis conditions on the formation of layered double hydroxides. *Journal of Solid State Chemistry* **269**, 494–506.

Cavani, F., Trifiro, F. & Vaccari, A. 1991 Hydrotalcite-type anionic clays: preparation, properties and applications. *Catalysis Today* **11** (2), 173–301.

Chitrakar, R., Tezuka, S., Sonoda, A., Sakane, K. & Hirotsu, T. 2008 A new method for synthesis of Mg-Al, Mg-Fe, and Zn-Al layered double hydroxides and their uptake properties of bromide ion. *Industrial & Engineering Chemistry Research* **47** (14), 4905–4908.

Chitrakar, R., Sonoda, A., Makita, Y. & Hirotsu, T. 2011 Calcined Mg-Al layered double hydroxides for uptake of trace levels of bromate from aqueous solution. *Industrial & Engineering Chemistry Research* **50** (15), 9280–9285.

Choi, H. 2017 Use of methyl esterified eggshell membrane for treatment of aqueous solutions contaminated with anionic sulfur dye. *Water Science and Technology* **76** (10), 2638–2646.

Chowdhury, P. R. & Bhattacharyya, K. G. 2015 Ni/Ti layered double hydroxide: synthesis, characterization and application as a photocatalyst for visible light degradation of aqueous methylene blue. *Dalton Transactions* **44** (15), 6809–6824.

Chuang, Y. H., Tzou, Y. M., Wang, M. K., Liu, C. H. & Chiang, P. N. 2008 Removal of 2-chlorophenol from aqueous solution by Mg/Al layered double hydroxide (LDH) and modified LDH. *Industrial & Engineering Chemistry Research* **47** (11), 3813–3819.

Fernandez, J. M., Ulibarri, M. A., Labajos, F. M. & Rives, V. 1998 The effect of iron on the crystalline phases formed upon thermal decomposition of Mg-Al-Fe hydrotalcites. *Journal of Materials Chemistry* **8** (11), 2507–2514.

Futalan, C. M., Kim, J. & Yee, J. 2019 Adsorptive treatment via simultaneous removal of copper, lead and zinc from soil washing wastewater using spent coffee grounds. *Water Science and Technology* **76** (6), 1029–1041.

Goh, K. H., Lim, T. T. & Dong, Z. 2008 Application of layered double hydroxides for removal of oxyanions: a review. *Water Research* **42** (6–7), 1343–1368.

Hu, E., Wu, X., Shang, S., Tao, X., Jiang, S. & Gan, L. 2016 Catalytic ozonation of simulated textile dyeing wastewater using mesoporous carbon aerogel supported copper oxide catalyst. *Journal of Cleaner Production* **112**, 4710–4718.

Hua, J. F., Zhang, M. D. & Huang, M. 2014 Effect of nano-Fe_2O_3/goldmine complex on dyeing wastewater treatment. *Advanced Materials Research* **955–959**, 335–338.

Islam, M. A., Sabar, S., Benhouria, A., Khanday, W. A., Asif, M. & Hameed, B. H. 2017 Nanoporous activated carbon prepared from karanj (*Pongamia pinnata*) fruit hulls for methylene blue adsorption. *Journal of the Taiwan Institute of Chemical Engineers* **74**, 96–104.

Kalalie, N., Wang, X. & Wang, D. Y. 2016 Synthesis of a Fe_3O_4 nanosphere@Mg-Al layered-double-hydroxide hybrid and application in the fabrication of multifunctional epoxy nanocomposites. *Industrial & Engineering Chemistry Research* **55** (23), 6634–6642.

Kannan, N. & Sundaram, M. M. 2001 Kinetics and mechanism of removal of methylene blue by adsorption on various carbons a comparative study. *Dyes and Pigments* **51** (1), 25–40.

Khorram, A. G. & Fallah, N. 2018 Treatment of textile dyeing factory wastewater by electrocoagulation with low sludge settling time: optimization of operating parameters by RSM. *Journal of Environmental Chemical Engineering* **6** (1), 635–642.

Konicki, W., Pełech, I., Mijowska, E. & Jasińska, I. 2012 Adsorption of anionic dye Direct Red 23 onto magnetic multi-walled carbon nanotubes-Fe_3C nanocomposite: Kinetics, equilibrium and thermodynamics. *Chemical Engineering Journal* **210**, 87–95.

Kumar, P. S., Ramalingam, S. & Sathishkumar, K. 2010 Removal of methylene blue dye from aqueous solution by activated carbon prepared from cashew nut shell as a new low-cost adsorbent. *Korean Journal of Chemical Engineering* **28** (1), 149–155.

Lan, M., Fan, G., Yang, L. & Li, F. 2014 Significantly enhanced visible-light-induced photocatalytic performance of hybrid Zn-Cr layered double hydroxide/graphene nanocomposite and the mechanism study. *Industrial & Engineering Chemistry Research* **53** (33), 12943–12952.

Lazaridis, N. K., Karapantsios, T. D. & Georgantas, D. 2003 Kinetic analysis for the removal of a reactive dye from aqueous solution onto hydrotalcite by adsorption. *Water Research* **37** (12), 3023–3033.

Lee, H. J., Halali, M. A., Sarathy, S. & Lannoy, C. F. 2020 The impact of monochloramines and dichloramines on reverse osmosis membranes in wastewater potable reuse process trains: a pilot-scale study. *Environmental Science: Water Research & Technology* **6**, 1336–1346. doi:10.1039/d0ew00048e.

Li, F. & Duan, X. 2005 Applications of layered double hydroxides. *Structure & Bonding* **119** (1), 193–223.

Li, Y., Zhang, Y., Zhang, Y., Wang, G., Li, S., Han, R. & Wei, W. 2018 Reed biochar supported hydroxyapatite nanocomposite: characterization and reactivity for methylene blue removal from aqueous media. *Journal of Molecular Liquids* **263**, 53–63.

Li, J., Wang, Q., Zheng, L. & Liu, H. 2020 A novel graphene aerogel synthesized from cellulose with high performance for removing MB in water. *Journal of Materials Science & Technology* **41**, 68–75.

Liang, Z., Wang, J., Zhang, Y., Han, C., Ma, S., Chen, J., Li, G. & An, T. 2020 Removal of volatile organic compounds (VOCs) emitted from a textile dyeing wastewater treatment plant and the attenuation of respiratory health risks using a pilot-scale biofilter. *Journal of Cleaner Production* **253**, 120019. doi:10.1016/j.jclepro.2020.120019.

Pan, T. D., Li, Z. J., Shou, D. H., Shou, W., Fan, J. T., Liu, X. & Liu, Y. 2019 Buoyancy assisted janus membrane preparation by ZnO interfacial deposition for water pollution treatment and self-cleaning. *Advanced Materials Interfaces* doi:10.1002/admi.201901130.

Rashidi, H. R., Sulaiman, N. M. N., Hashim, N. A., Hassan, C. R. C. & Ramli, M. R. 2014 Synthetic reactive dye wastewater treatment by using nano-membrane filtration. *Desalination and Water Treatment* **55** (1), 86–95.

Rengaraj, S., Kim, Y., Joo, C. K. & Yi, J. 2004 Removal of copper from aqueous solution by aminated and protonated mesoporous aluminas: kinetics and equilibrium. *Journal of Colloid & Interface Science* **273** (1), 14–21.

Salleh, M. A. M., Mahmoud, D. K., Karim, W. A. W. A. & Idris, A. 2011 Cationic and anionic dye adsorption by agricultural solid wastes: a comprehensive review. *Desalination* **280** (1–3), 1–13.

Selvam, K., Swaminathan, K. & Chae, K. S. 2003 Decolourization of azo dyes and a dye industry effluent by a white rot fungus *Thelephora* sp. *Bioresource Technology* **88** (2), 115–119.

Thi, H. T., Hoang, A. L., Huu, T. P., Dinh, T. N., Chang, S. W., Chung, W. J. & Nguyen, D. D. 2020 Adsorption isotherms and kinetic modeling of methylene blue dye onto a carbonaceous hydrochar adsorbent derived from coffee husk waste. *Science of The Total Environment* **725**, 138325. doi:10.1016/j.scitotenv.2020.138325.

Wang, Y. & Gao, H. 2006 Compositional and structural control on anion sorption capability of layered double hydroxides (LDHs). *Journal of Colloid & Interface Science* **301** (1), 19–26.

Wang, Q., Undrell, J. P., Gao, Y., Cai, G. P., Buffet, J., Wilkie, C. A. & O'Hare, D. 2013 Synthesis of flame-retardant polypropylene/LDH-borate nanocomposites. *Macromolecules* **46** (15), 6145–6150.

Xia, S. J., Liu, F. X., Ni, Z. M., Shi, W., Xue, J. L. & Qian, P. P. 2014 Ti-based layered double hydroxides: efficient photocatalysts

for azo dyes degradation under visible light. *Applied Catalysis B: Environmental* **144**, 570–579.

Xie, Y., Ye, G. Q., Peng, S. P., Jiang, S. Y., Wang, Y. & Hu, X. Y. 2019 Postsynthetic functionalization of water stable zirconium metal organic frameworks for high performance copper removal. *Analyst* **144**, 4552–4558. doi:10.1039/C9AN00981G.

Yang, C. A., Huang, H., Ji, T., Zhang, K., Yuan, L., Zhou, C., Tang, K., Yi, J. & Chen, X. 2019 A cost-effective crosslinked β-cyclodextrin polymer for the rapid and efficient removal of micropollutants from wastewater. *Polymer International* **68** (4), 805–811. doi.org/10.1002/pi.5771.

Yu, J., Martin, B. R., Clearfield, A., Luo, Z. & Sun, L. 2015 One-step direct synthesis of layered double hydroxide single-layer nanosheets. *Nanoscale* **7** (21), 9448–9451.

Zhao, J., Huang, Q., Liu, M., Dai, Y., Chen, J., Huang, H., Wen, Y., Zhu, X., Zhang, X. & Wei, Y. 2017 Synthesis of functionalized MgAl-layered double hydroxides via modified mussel inspired chemistry and their application in organic dye adsorption. *Journal of Colloid and Interface Science* **505**, 168–177.

Zhou, C. H., Beltramini, J. N., Lin, C. X., Xu, Z. P., Lu, G. Q. & Tanksale, A. 2011 Selective oxidation of biorenewable glycerol with molecular oxygen over Cu-containing layered double hydroxide-based catalysts. *Catalysis Science & Technology* **1**, 111–122.

Zollinger, H. 1989 Color chemistry: synthesis, properties and applications of organic dyes and pigments. *Leonardo* **22** (3–4), 313–314.

First received 9 March 2020; accepted in revised form 18 June 2020. Available online 6 July 2020